

# RSC Advances



This is an *Accepted Manuscript*, which has been through the Royal Society of Chemistry peer review process and has been accepted for publication.

*Accepted Manuscripts* are published online shortly after acceptance, before technical editing, formatting and proof reading. Using this free service, authors can make their results available to the community, in citable form, before we publish the edited article. This *Accepted Manuscript* will be replaced by the edited, formatted and paginated article as soon as this is available.

You can find more information about *Accepted Manuscripts* in the [Information for Authors](#).

Please note that technical editing may introduce minor changes to the text and/or graphics, which may alter content. The journal's standard [Terms & Conditions](#) and the [Ethical guidelines](#) still apply. In no event shall the Royal Society of Chemistry be held responsible for any errors or omissions in this *Accepted Manuscript* or any consequences arising from the use of any information it contains.

Cite this: DOI: 10.1039/c0xx00000x

www.rsc.org/xxxxxx

ARTICLE TYPE

# Identification of a Small Molecule Preventing BMSC Senescence *in vitro* by Improving Intracellular Homeostasis via ANXA7 and Hmbox1

Fang-Wu Wang<sup>a</sup>, Fei Zhao<sup>a</sup>, Xing-Yang Qian<sup>a</sup>, Zhe-Zhen Yu<sup>a</sup>, Jing Zhao<sup>a</sup>, Le Su<sup>a</sup>, Yun Zhang<sup>b</sup>, Shang-Li Zhang<sup>a</sup>, Bao-Xiang Zhao<sup>c,\*</sup> and Jun-Ying Miao<sup>a,b,\*</sup>

Received (in XXX, XXX) Xth XXXXXXXXX 20XX, Accepted Xth XXXXXXXXX 20XX

DOI: 10.1039/b000000x

Recently chemical small molecules have been proved an ideal and promising intervention for bone marrow-derived mesenchymal stem cell (BMSC)-based tissue regeneration therapies. In this study, we discovered the huge anti-aging potential of a bioactive small molecule, 6-amino-3,4-dihydro-2H-3-hydroxymethyl-1,4-benzoxazine (ABO), which can suppress a series of senescent phenotypes, enhancing proliferation and differentiation capacities in cultured rat BMSCs. We further illustrated that those beneficial effects were attributed to an improvement of cellular homeostasis, from intracellular degradation system to cytoskeleton organization. ABO could enhance autophagy and reduce intracellular oxidative stress, by facilitating lysosomal degradation. The direct target protein of ABO, ANXA7, was elevated and essential for autophagy induction and lysosomal protection against Baf-A1 upon ABO treatment. Hmbox1 was another critical protein elevated by ABO and probably downstream ANXA7. Intriguingly, the subcellular distribution of Hmbox1 was largely overlapped with cytoskeletal microfilaments and this might lead to a microfilament reorganization. ABO could decrease the level of Caveolin-1, indicating a remodeling in F-actin assembly and attracted our interest to investigate the interaction between Hmbox1, Caveolin-1 and ANXA7 in microfilament formation at cell membrane in the future study.

## Introduction

The application of bone marrow-derived mesenchymal stem cells (BMSCs) in clinical infusion is now providing a great hope for cell therapies and tissue engineering in a wide variety of diseases.<sup>1-3</sup> However, BMSCs cultured *in vitro* possess a very limited proliferation potential, with a maximum of about 40 PD for young donors and a sharp decline to 20 PD for older donors,<sup>4,5</sup> substantially restricting the effect and efficiency of clinical treatment, especially impeding development of autologous cell-based therapy for senior patients. Therefore, more information about molecular mechanisms of BMSC senescence and potential intervention strategies would greatly benefit augmentation of tissue regeneration therapies utilizing BMSCs.

Although accumulative reports have recognized a series of cellular or molecular markers of senescent BMSCs, e.g., loss of proliferation and multipotentiality,<sup>4,6</sup> enlarged morphology,<sup>7</sup> telomere attrition,<sup>5</sup> elevated level of p53 and p21,<sup>8</sup> decreased antioxidants and stress resistance,<sup>8,9</sup> downregulated DNA damage repair genes,<sup>10</sup> etc., the deep mechanisms regarding the onset and effect of BMSC senescence still remain poorly understood. Senescent phenotypes in long-lived cells are often consequences

of collapsed homeostasis, leading to accumulation of insoluble protein aggregates, lipofuscin, dysfunctional organelles and increased DNA damages. Currently, an important intracellular degradation and homeostasis maintenance system, autophagy, has attracted rapidly growing attentions to its intrinsic link with aging.<sup>11</sup> With the ability of "cleansing" and rejuvenating cellular components, autophagy is suggested to be a critical anti-oxidant mechanism.<sup>12</sup> However, autophagic degradation is paradoxically susceptible to oxidative impairments during aging, and a decline of autophagic activity with age has been depicted in almost all tissues and organisms analyzed.<sup>13</sup> Studies indicated that accumulation of undigested products inside lysosomes, usually in the form of heavy lipofuscin loading, appeared to cause severe oxidative impairments to lysosomes, which was a primary cause for compromising autophagic degradation in aging cells.<sup>14</sup> Although autophagy in BMSCs has remained largely uncharacterized, several studies suggested that autophagy protected BSMCs from oxidative stress,<sup>15</sup> hypoxia,<sup>16</sup> serum deprivation<sup>17</sup> and X-ray radiation.<sup>18</sup> It is possible that autophagy may play a similar role in the maintenance of BMSCs as other long-lived cells.<sup>19</sup>

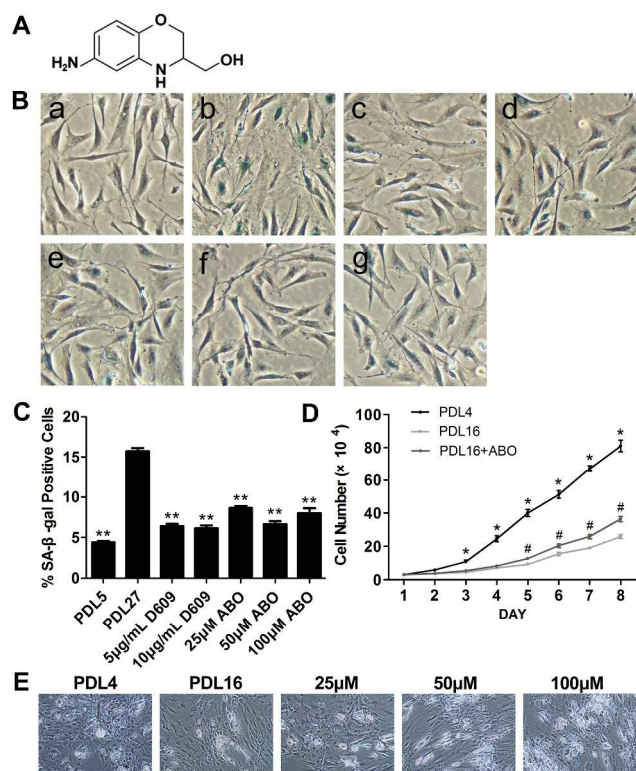


**Fig. 1 Senescence-associated markers showed ABO suppressed cellular aging in BMSCs.** A: The chemical structure of ABO, 6-amino-3,4-dihydro-2H-3-hydroxymethyl-1,4-benzoxazine. B: SA-β-Gal activity and morphology of young (PDL 5) and senescent (PDL 27) BMSCs. a, b: Normal BMSCs at PDL 5 and PDL 27. c, d: Senescent BMSCs treated with 5 μg/mL, 10 μg/mL D609 for 24 h, as positive control. e - g: Senescent BMSCs treated with 25 μM, 50 μM, 100 μM ABO for 24 h. C: Percentage of SA-β-Gal-positive cells. (\*\*P < 0.01 versus PDL 27 cells, results were expressed as mean ± SEM, n = 3). D: Growth curves of BMSCs at PDL 4, PDL 16 and PDL 16 with 50 μM ABO. (\*P < 0.05; #P < 0.05 versus PDL 16 cells, results were expressed as mean ± SEM, n = 4.). E: Effect of ABO on adipogenic differentiation capacity, manifested by morphology of BMSCs at PDL 4, PDL 16, and PDL 16 with ABO treatment.

So far, attempts to delay BMSC senescence for reaching a higher expansion level *in vitro* have been mainly concentrating on supplementation of various growth factors and cytokines. However, most of these factors stimulate cell proliferation via activating growth signaling pathways,<sup>20</sup> which are not able to essentially improving disturbed cellular homeostasis in aging cells, and worse still, may draw into undesirable effects such as cancer, metastasis and fibrosis.<sup>21,22</sup> Enhancing telomerase activity by introduction of lentivirus-mediated hTERT is also an approach.<sup>23,24</sup> However, there still exist safety concerns about the usage of viral vectors as well as tumorigenesis risk of telomerase over-activation. Recently, several studies have shed light on the identification and development of bioactive small molecules to facilitate differentiation of BMSCs *in vitro* in cell-based regenerative medicine field.<sup>25-27</sup> Small chemicals have some unique advantages, e.g., they can specifically target certain pathways related to selective cellular functions, thus the side effects can be minimized. Also, the production and preservation of chemicals is much less costly compared to growth factors. Even though small molecules have become an ideal intervention approach in regeneration medicine, anti-aging small molecules in BMSCs have been rarely announced.<sup>28</sup> Herein, we reported a

bioactive small molecular compound, 6-amino-3,4-dihydro-2H-3-hydroxymethyl-1,4-benzoxazine (ABO), could effectively inhibit cell senescence in cultured rat BMSCs.

Our previous studies illustrated multifunctions of ABO in several cell lineages, highlighting its roles in stimulating mTOR-independent autophagy,<sup>29, 30</sup> promoting angiogenesis, inhibiting apoptosis,<sup>31, 32</sup> modulating differentiation,<sup>27, 33</sup> etc.. While it was the first time to demonstrate the anti-senescence effect of ABO. We utilized cultured rat BMSCs of different population doubling levels (PDLs), a Hayflick model of replicative senescence,<sup>34</sup> for initial investigations to illustrate the underlying molecular mechanisms. We found ABO improved cellular homeostasis in senescent BMSCs, primarily by activating autophagy and enhancing cytoskeleton homeostasis.

## Results and discussion

### ABO inhibited cultured BMSC senescence

We discovered that ABO treatment significantly suppressed senescent biomarkers in BMSCs (Fig. 1). SA-β-gal staining result showed an increased proportion of positively stained cells in senescent group (PDL 27) compared to PDL 5, with an obvious morphological change (Fig. 1B). The morphology of senescent cells were more flat and spreading, with increased podia and actin stress filaments,<sup>4</sup> in contrast to spindle-type morphology of young cells. We found ABO-treated senescent cells exhibited a significantly decreased number of SA-β-gal positive cells, comparable to the positive control, the anti-aging chemical D609<sup>28</sup> (Fig. 1B, C). Moreover, ABO-treated cells adopted a thinner and smaller morphology, with less cytoplasmic extensions and actin filaments. To investigate the influence of ABO on cell growth kinetics, the total cell number of each group was tracked starting at  $2 \times 10^4$  for consecutive 8 days (Fig. 1D). We found the growth curve of ABO-treated PDL 16 cells presented a higher slope, indicating a faster proliferation speed. Although there were discrepancies on adipocytic differentiation potential with age *in vivo*,<sup>35, 36</sup> numerous studies demonstrated that cultured BMSCs gradually lost their adipogenic potential.<sup>4, 8, 37</sup> In this study, BMSCs at different PDLs were cultured for 10 days in adipogenic medium. A decline of differentiation capacity was observed in senescent cells, while senescent cells incubated with adipocyte medium containing 50 μM ABO presented a higher number of adipocytes, reflecting an enhanced differentiation potential (Fig. 1E). Intensified oxidative stress is a remarkable feature of senescent phenotypes. We also observed that ABO treatment could appreciably diminish intracellular ROS to a level similar to young cells (Fig. S1†). From these results, it would be safe to infer that ABO suppressed BMSC aging *in vitro*, with a huge potential to restore its proliferation and differentiation capacities.

### ABO-induced autophagy and the target protein ANXA7 were crucial for senescence inhibition in BMSCs

ABO had been demonstrated as a robust mTOR-independent autophagy inducer in our previous studies<sup>29, 30</sup>. Immunoblotting of LC3 (microtubule-associated protein 1 light chain 3), an established marker of autophagy, showed a decreased level of autophagy in senescent cells, and ABO treatment significantly restored the autophagic activity (Fig. 2A). A complete autophagic



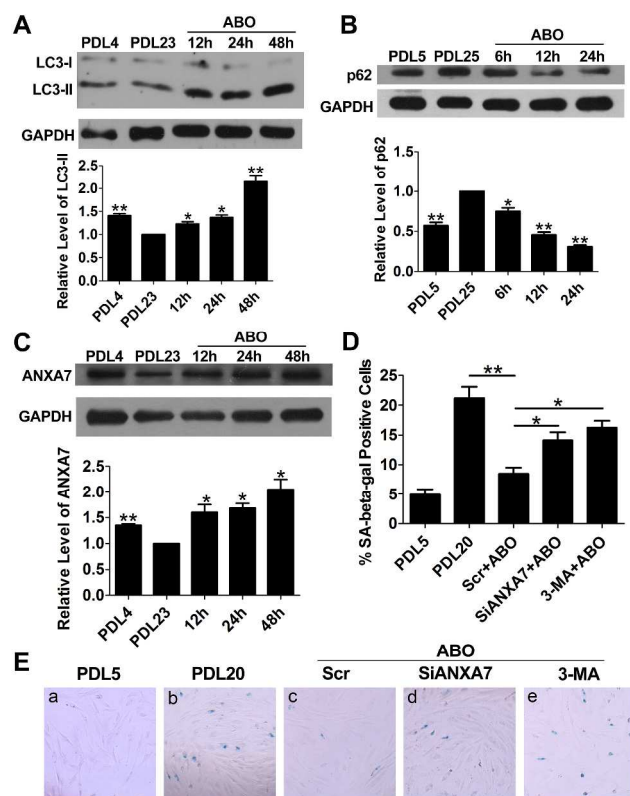


**Fig. 2** ABO-induced autophagy and ANXA7 contributed to the anti-senescent effect of ABO. A: Western blot assay of LC3-II indicated a decline of autophagy with age. ABO enhanced autophagic activity in senescent BMSCs. B: Western blot assay of p62 suggested ABO promoted clearance of p62 by autophagy in senescent cells. C: The level of ANXA7 decreased with age, and prominently elevated by ABO in senescent BMSCs. D, E: SA- $\beta$ -Gal staining implied that upregulated ANXA7 and autophagy were indispensable for senescence inhibition in BMSCs. a, b: normal BMSCs at PDL 5 and PDL 20. c - e: PDL 20 cells respectively subject to 20 nM scrambled siRNA, 20 nM ANXA7 siRNA and 5 mM 3-MA, for 12 h and then incubated with culture medium containing 50  $\mu$ M ABO for 48 h. The percentage of SA- $\beta$ -Gal-positive cells was measured in (D) (\*\*  $p < 0.01$ , \*  $p < 0.05$ , results were expressed as mean  $\pm$  SEM,  $n = 3$ ).

flux and efficient autophagic degradation was further validated by p62/SQSTM1 protein level (Fig. 2B). As a ubiquitin-binding adaptor protein for both proteasome and autophagy pathways, p62 and the targeted cargos become incorporated into autophagosomes. We monitored a high amount of p62 accumulated in senescent cells, and ABO prominently reduced p62 level through autophagic degradation. Currently p62 has become a novel target for aging studies, as a key effector in protein homeostasis, nutrient signalings, antioxidant responses, etc.<sup>38</sup> Our result indicated that ABO might have an influence on the biofunctions of p62, particularly protein homeostasis via modulating autophagy.

ANXA7, a direct target protein of ABO, was discovered to participate in ABO induced autophagy<sup>30</sup>. In this study, we also found ANXA7 was raised by ABO in senescent BMSCs (Fig. 2C). Interestingly, ANXA7 gradually declined with age, suggesting a potent role in the aging mechanism. To confirm whether upregulated autophagy and ANXA7 were indispensable for senescence inhibition by ABO, we conducted SA- $\beta$ -gal staining

after subjecting cells to ANXA7 siRNA and autophagy inhibitor, 3-MA, concurrent with ABO treatment. The result indicated that both ANXA7 silencing and autophagy cutoff significantly suppressed reduction of SA- $\beta$ -gal activity by ABO (Fig. 2D, E), thus they were indicated indispensable for the anti-aging effect of ABO.

#### ABO protected and enhanced lysosomal activity via ANXA7

The blockage of lysosomal degradation, the last step of autophagy, would result in accumulation of giant autolysosomes and subversion of autophagy.<sup>39</sup> During aging, lysosomal membrane permeabilization and integrity are perturbed,<sup>40</sup> leading to a rapid collapse of lysosomal pH and intracellular digestion. We wondered whether ABO-induced autophagy was a consequence of enhanced lysosomal degradation. Acridine orange (AO) is commonly used as an indicator for changes in lysosomal pH, lysosomal integrity and permeability.<sup>41, 42</sup> As determined by AO staining (Fig. 3A), senescent cells at PDL 20 displayed a dim and dispersed red fluorescence compared to the red punctuated fluorescence signal in young cells. ABO treatment greatly increased red puncta inside senescent cells, indicating a higher level of lysosomal activity. However, this effect was attenuated by ANXA7 silencing.

We next utilized Bafilomycin-A1 (Baf-A1), a recognized inhibitor of vacuolar H<sup>+</sup>-ATPase (V-ATPase) located on lysosomal membrane, to investigate whether ABO functioned by maintaining lysosomal pH gradient. By exposing cells to 20 nM Baf-A1 for 8 h, we found the red fluorescence nearly disappeared in control cells (Fig. 3Ae). When cells were pre-treated with 50  $\mu$ M ABO for 24 h, and then exposed 20 nM Baf-A1 supplemented with ABO for 8 h, the red acidic compartments were significantly retained, indicating ABO could counteract Baf-A1 impairment (Fig. 3Af). However, ANXA7 knockdown almost abolished this protective effect (Fig. 3Ag), thus we hypothesized that ANXA7 might be a key factor in lysosomal activity recovery upon ABO treatment. To further illustrate this, we examined subcellular distribution of ANXA7 and lysosomes by immunofluorescence. As shown in Fig. 3B, ABO significantly elevated the level of ANXA7 and altered its distribution pattern inside senescent cells, with an obviously increased co-localization between ANXA7 and lysotracker, a pH-dependent probe for lysosomes. After incubation with Baf-A1 for 1 h, the signal of lysotracker was nearly diminished. ABO pre-treatment for 24 h could ameliorate lysosomal impairment by Baf-A1 (Fig. 3B), accompanied by a superposition of ANXA7 puncta and lysosomes, which indicated ANXA7 might interact directly with lysosomes.

#### ABO upregulated Hmbox1 in senescent BMSCs via ANXA7

Besides ANXA7, we discovered that ABO raised the level of Hmbox1 in senescent BMSCs, a recently-identified transcription factor belonging to hepatocyte nuclear factor of Homeobox family. As shown in Fig. 4A, Hmbox1 also strikingly declined with age. ABO treatment could upregulate Hmbox1 by up to 2-3 fold at 6 h. However, elevation of Hmbox1 level only sustained a short time period within 24 h, reflecting the existence of a sophisticated regulation network drawing Hmbox1 to a normal level. So far, there has been no report regarding the upstream

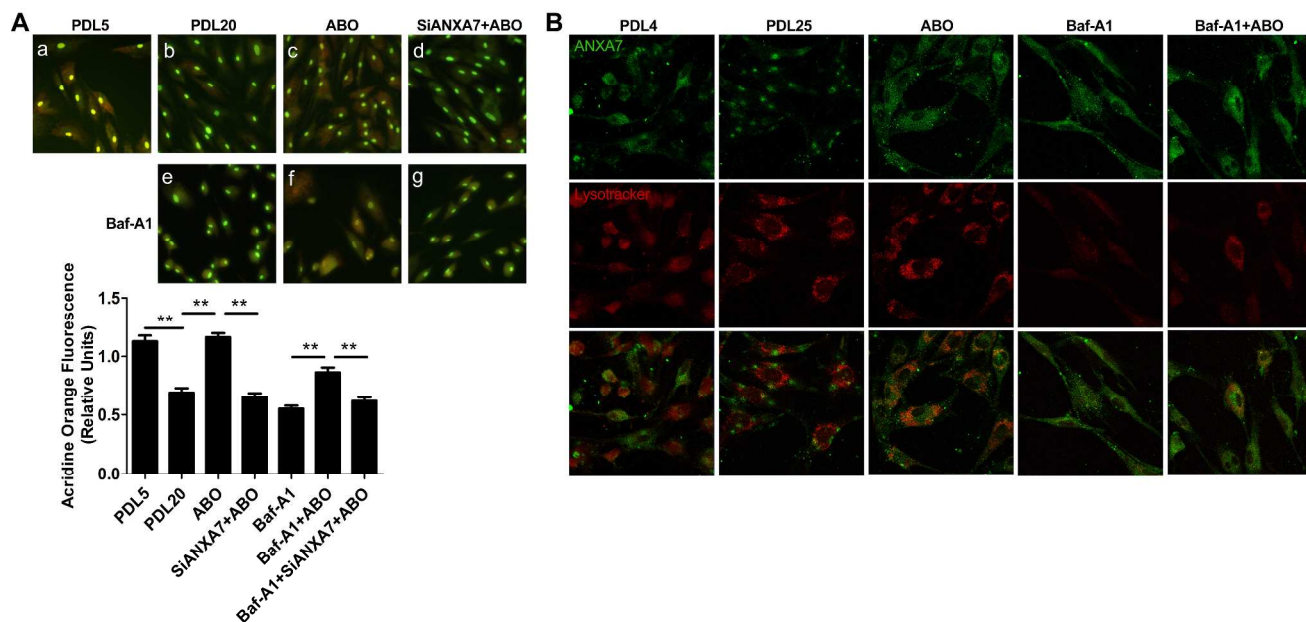


**Fig. 3** ABO promoted lysosomal degradation and protected lysosomes from Baf-A1 impairment via ANXA7. A: Acridine Orange staining for young and senescent BMSCs. a-d: Lysosomal activity declined with age as shown in (a) and (b). 50  $\mu$ M ABO treatment for 24h significantly restored the amount of acidic vacuoles (c), but this effect diminished when cells were subject to 20 nM ANXA7 siRNA before ABO treatment (d). e-g: BMSCs were exposed to 20 nM Baf-A1 for 8 h with (f) or without (e) pre-incubation with ABO for 24 h. ANXA7 silencing attenuated the protective effect of ABO (g). The fluorescence was quantified in the below panel (\*\*  $p < 0.01$ , results were expressed as mean  $\pm$  SEM,  $n = 3$ ). B: ABO altered subcellular distribution pattern of ANXA7 and increased co-localization between ANXA7 and lysosomes. 20 nM Baf-A1 treatment for 1 h severely impaired lysosomes, while ABO pre-treatment for 24 h counteracted the damaging effect.

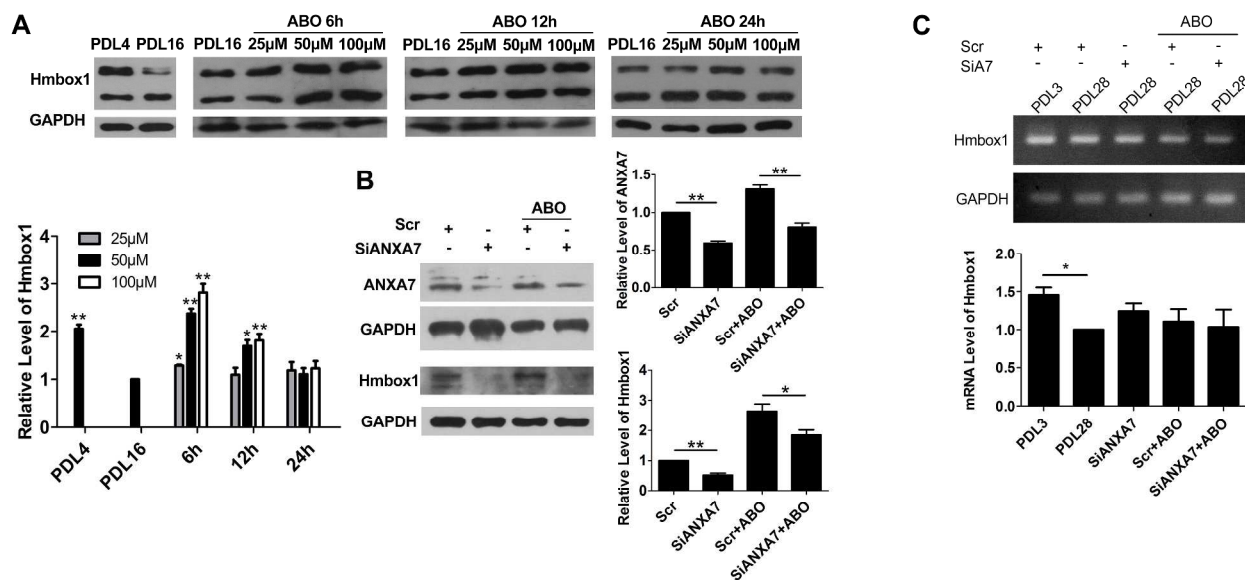


**Fig. 4** ABO upregulated Hmbox1 in senescent BMSCs via ANXA7. A: Western blot analysis showed that Hmbox1 level declined with age and upregulated by ABO prominently at 6 h and 12 h, then returned to a normal level at 24 h (\* $p < 0.05$ , \*\* $p < 0.01$  versus PDL 16, results were expressed as mean  $\pm$  SEM,  $n = 4$ ). B: ANXA7 silencing dramatically decreased Hmbox1 protein, and prevented upregulation of Hmbox1 by ABO (\* $p < 0.05$ , \*\* $p < 0.01$ , results were expressed as mean  $\pm$  SEM,  $n = 5$ ). C: The relative mRNA level of Hmbox1 was evaluated by RT-PCR. Although young cells exhibited higher amount of Hmbox1 mRNA than senescent cells, there was no apparent difference between normal and ANXA7 silencing groups (\* $p < 0.05$ , results are expressed as mean  $\pm$  SEM,  $n = 3$ ).

regulatory mechanism of Hmbox1. By performing ANXA7 silencing, we found that knockdown of ANXA7 dramatically decreased Hmbox1 protein in untreated cells and nearly offset elevating effect by ABO (Fig. 4B). To figure out whether ANXA7 affected Hmbox1 at transcription or post-transcription level, we

also analyzed the mRNA changes of Hmbox1, but there was no significant difference between normal and ANXA7 silencing groups in senescent BMSCs (Fig. 4C). Thus, ANXA7 might serve as an upstream regulator of Hmbox1 at post-transcriptional level.

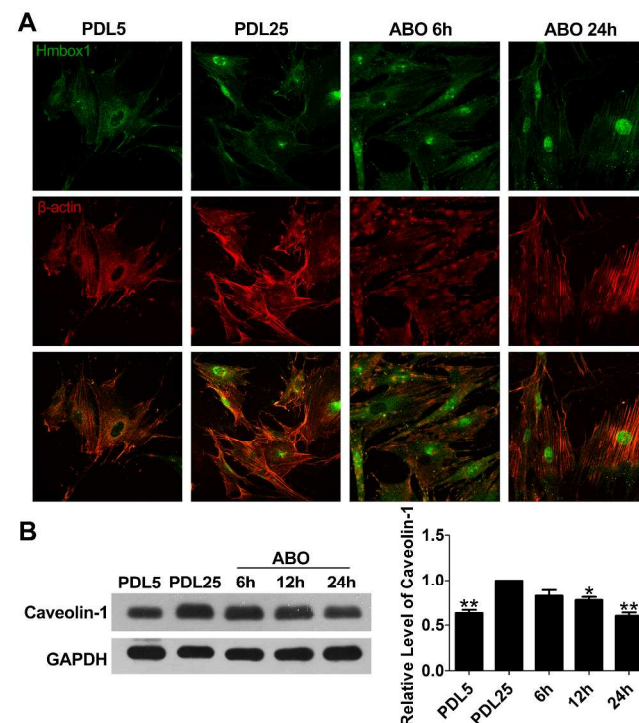


**Fig. 5** The subcellular distribution of Hmbox1 co-localized with cytoskeletons and might engage in microfilament reorganization. A: Hmbox1 was largely overlapped with microfilaments marked by  $\beta$ -actin protein, and both Hmbox1 and the architecture of microfilament underwent redistribution upon ABO treatment. B: Western blot analysis showed Caveolin-1 increased with age and was downregulated by ABO at 24 h (\* $p < 0.05$ , \*\* $p < 0.01$ , results were expressed as mean  $\pm$  SEM,  $n = 3$ ).

#### Hmbox1 was important for microfilament organization in senescent BMSCs

We next performed Hmbox1 silencing and overexpression experiments and observed the impact of Hmbox1 protein on cellular senescent state by SA- $\beta$ -gal staining. We found knockdown of Hmbox1 appreciably suppressed anti-aging effect of ABO, whereas its overexpression by transfecting pCMV-Hmbox1 greatly reduced positively stained cells (Fig. S2<sup>†</sup>), suggesting that Hmbox1 was a senescence-associated factor and at least in part mediated the anti-aging effect of ABO.

Since identified in 2006,<sup>43</sup> the biological functions of Hmbox1 has been gradually uncovered in the past several years, particularly in immunology,<sup>44, 45</sup> cell differentiation,<sup>27</sup> telomere extension.<sup>46, 47</sup> Although the intriguing functions of Hmbox1 in telomere greatly attracted our attention, we proposed that this function was unlikely to exert an immediate effect within 24 h when ABO already had reversed some of the senescent phenotypes. We examined the subcellular distribution of Hmbox1 and found surprisingly that it displayed paralleled string-like filaments throughout the cell, resembling the morphology of cytoskeletons. Then we conducted co-immunostaining of Hmbox1 with  $\beta$ -actin and  $\alpha$ -tubulin respectively, to make clear whether Hmbox1 interacted with microfilaments or microtubules. As a result, Hmbox1 perfectly overlapped with microfilaments (Fig. 5A), while only partially co-localized with microtubules labeled by  $\alpha$ -tubulin, with no apparent change after ABO treatment (data not shown). As shown in Fig 5B, ABO

significantly elevated the protein level of Hmbox1 at 6 h, and caused an obvious change in microfilament architecture at 6 h and 24 h. The structure of microfilaments in senescent cells appeared to be denser and more chaotic than that of young cells and typically presented higher concentration at the periphery of cells. However, after ABO treatment, the arrangement of microfilaments tended to be more paralleled and monodirectional, with a larger proportion of microfilaments distributed in cytosol instead of the edge of the cell. We speculated those changes could account for a thinner and less spreading morphology of ABO-treated cells (Fig 1A). According to previous studies, the morphological and mobility changes in aging cells are mainly attributed to the organization and dynamics of microfilaments.<sup>48</sup> Several studies demonstrated that microfilaments in senescent cells had an increased rigidity and a declined turnover rate.<sup>49, 50</sup> In this study, we hypothesized that the changes in morphology (Fig. 1B) and microfilament organization caused by ABO was mediated by Hmbox1, given its significant upregulation at 6 h and an apparent co-localization with filamentous actins (F-actins). But the underlying mechanisms of whether and how Hmbox1 participated in microfilament remodeling and turnover remained to be examined.

F-actins are basically nucleated at the cell membrane and usually anchored to focal adhesions, connecting microfilaments to extracellular matrix.<sup>51</sup> In human diploid fibroblasts, increased formation of focal adhesions led to the senescent phenotype of microfilaments, and Caveolin-1 facilitated this process by interacting with focal adhesion kinase which regulated actin stress fiber formation.<sup>52</sup> By Caveolin-1 immunoblotting, we found senescent cells had elevated Caveolin-1 level, which could be reduced by ABO treatment to a level akin to young cells (Fig. 5B). We then proposed the potential function of Hmbox1 in microfilament remodeling perhaps associated with Caveolin-1 and F-actin formation at cell membrane. Whether Hmbox1 could interact with Caveolin-1 and remodel F-actin assembly is an intriguing topic in the following study.

## Experimental

### Cell Culture

Rat bone marrow collection and mesenchymal stem cell isolation were performed according to Pittenger et al.<sup>53</sup> In brief, bone marrow in the femurs and tibias of male Wistar rats (90 - 100 g) was washed using Dulbecco's modified Eagle's medium-low glucose (DMEM-LG) (Gibco) supplemented with 10% FBS (Gibco). BMSCs were isolated by removal of non-adherent cells after 72 h and the medium was changed every 2 days until adherent cells reached 50 % confluence and harvested with 0.05 % trypsin (Sangon Biotech) in phosphate-buffered saline (PBS). Cells were grown to 70 - 80 % confluence and then passaged or seeded in plates or appropriate dishes at a density of 5000  $\text{cm}^{-2}$ . The experiments were conducted on cells at varied PDLs to demarcate young (PDL 3-5) and senescent (PDL 16-30) BMSCs.

### Cell Treatment

ABO was synthesized as reported with purity greater than 98 % and the structure was confirmed by spectral data.<sup>31</sup> ABO was dissolved in dimethylsulfoxide (DMSO) to make a 0.1 M stock solution. BMSCs were incubated with culture medium containing



25  $\mu\text{M}$ , 50  $\mu\text{M}$ , 100  $\mu\text{M}$  ABO, or corresponding volume of DMSO solvent as control (below 0.1 %, v / v) in all subsequent experiments.

#### 5 Senescence-associated $\beta$ -galactosidase Assay

BMSCs seeded in 24-well plate were exposed to 2 % formaldehyde/0.5 % glutaraldehyde for fixation. After 5 min, cells were rinsed with PBS and warmed  $\beta$ -gal buffer solution (5 mM potassium ferrocyanide, 5 mM potassium ferricyanide, 10 mM NaCl, and 2 mM  $\text{MgCl}_2$ , pH = 6.0) for 1 min. Then cells were incubated with staining solution (buffer solution supplemented with 1 mg/mL 5-Bromo-4-chloro-3-indolyl  $\beta$ -D-galactopyranoside, Takara) for over 18 h at 37 °C. Senescent cells were stained blue under a phase-contrast microscopy. The percentage of positively stained cells was estimated by counting at least 1500 cells for each sample.

#### Growth Kinetics Assay

$2 \times 10^4$  cells were seeded in each dish (35 mm) at first and the number of cells was counted by cytometry using a hemacytometer after suspension of cells with 0.05 % trypsin. The culture medium was replaced every day and the ABO-treated group was incubated with medium containing 50  $\mu\text{M}$  ABO throughout 8 days.

#### *In vitro* Adipogenic Differentiation

Cells in 6-well plates were cultured in adipogenic induction medium (DMEM-LG supplemented with 10 % FBS, 0.01 mg/mL insulin, 1mM dexamethasone, 0.2 mM indomethacin and 0.5 mM 3-isobutyl-1-methylxanthine) for 10 days as previously described.<sup>28</sup> The induction medium was replaced every day. After 10 days, morphological changes were monitored under a phase-contrast microscopy.

#### 35 Western Blot

Protein SDS-PAGE and western blot were performed as previously reported.<sup>54</sup> Briefly, the total protein extracts were obtained in protein lysis buffer with 1 mM PMSF and boiled for 5 min in loading buffer. Equal amount of protein of each sample was loaded on 15 % SDS-polyacrylamide gel and underwent electrophoresis. Then the gel was electroblotted onto polyvinylidene difluoride membrane (Millipore, USA). After blocked with 5 % non-fat milk for 1 h, the membrane was probed with primary antibodies (1:1000 in 3 % BSA ) at 4 °C overnight, then horseradish peroxidase-conjugated secondary antibodies (1:5000 in 3 % non-fat milk), and detected with an enhanced chemiluminescence detection kit (Thermo Fisher, 34080). The relative quantities of protein bands were analyzed by Image-J software and normalized to loading control.

#### Intracellular ROS Level Detection

Intracellular ROS in BMSCs were detected using a fluoroprobe, DCHF (2',7'-dichlorodihydrofluorescein), which could transform into a highly fluorescent DCF (2',7'-dichlorofluorescein) when oxidized by ROS. BMSCs grown in 24-well plate were incubated with medium containing 5  $\mu\text{M}$  DCHF at 37 °C for 30 min and monitored under a confocal laser scanning microscope (Leica) with an excitation wavelength of 488 nm. The amount of ROS

was quantified as the relative fluorescence intensity of DCF per cell by Leica Confocal Software (LCS Lite).

#### Lysosomal Activity Detection

Lysosomal activity was monitored by use of a metachromatic fluorophore acridine orange (0.1 mg/mL). After treatment, BMSCs were gently rinsed twice with PBS and then subject to acridine orange staining for 5 min. Cells were washed in PBS and the fluorescence was observed under an inverted fluorescence microscope (Nikon).

#### 70 Immunofluorescence Microscopy

For immunofluorescence assay, BMSCs were seeded into glass bottom dishes (20 mm) and grown to 70 % confluence. After treatment, cells were fixed in 4 % paraformaldehyde for 15 min and blocked with goat serum (1:30 dilution in 0.1 M PBS) in 0.1 M PBS for 45 min at room temperature. Then cells were incubated with primary antibody (1:100 dilution) overnight at 4 °C and then with Alexa 488 or 546-labeled species-specific secondary antibodies (1:200 dilution in 0.1 M PBS) for 45 min at 37 °C. Finally cells were rinsed in 0.1 M PBS, and monitored by a confocal laser scanning microscope (Zeiss).

#### RNA Interference

Transfection of a specific siRNA targeting ANXA7 and Hmbox1 was facilitated by HiperFect RNA interference reagent, according to the manufacturer's instructions. BMSCs grown in 24-well plate and reached 60 % confluence were transfected with ANXA7 siRNA or Hmbox1 siRNA, and scrambled siRNA as negative control. After incubation with siRNAs for 12 h, the medium was substituted for normal culture medium and cells were ready for subsequent experiments. The efficiency of silencing was evaluated by western blot assay (Fig. S3<sup>†</sup>).

#### RT-PCR

RT-PCR analysis of Hmbox1 and GAPDH in BMSCs was conducted according to previously reported.<sup>27</sup> Total RNA of BMSCs were extracted and isolated by use of TRIzol reagent (Life Technologies) and an amount of 1  $\mu\text{g}$  of total RNA was reverse-transcribed using PrimeScript RT reagent Kit with gDNA Eraser (DRR047A, Takara). Synthesized complementary DNA was augmented by PCR utilizing 2 $\times$ EasyTaq PCR SuperMix (Transgen Biotech). The primer sequences were for Hmbox1, sense 5'-GTC CAG GAG GCC ATT CCA ACA GCG-3', antisense 5'-AAT GAG GGC ACC ATG CCA TCT TC-3'; and GAPDH as a normalization control, sense 5'-TAT CGG ACG CCT GGT TAC-3', antisense 5'-TGA GCC CTT CCA TAT GC-3'.

#### Antibodies

Antibodies for ANXA7 (sc-11389), Hmbox1 (sc-87768), GAPDH (sc-47724) and horseradish peroxidase-conjugated secondary antibodies were obtained from Santa Cruz Biotechnology. Antibodies for LC3 (2775) and Caveolin-1 (3238) were purchased from Cell Signaling Technology. Antibody for  $\beta$ -actin (A5441) was obtained from Sigma-Aldrich. Antibody for p62/SQSTM1 (PM045) was bought from MBL. Antibody for  $\alpha$ -tubulin (BM1452) was purchased from Boster, China. Secondary antibodies for immunofluorescence were donkey anti-rabbit IgG

Alexa Fluor-488 (Invitrogen, A21206) and goat anti-mouse IgG Alexa Fluor-546 (Invitrogen, A11003).

### Statistical Analysis

Data were presented as means  $\pm$  SE from at least three independent experiments and analyzed by Student's t-test. Differences at  $p < 0.05$  were considered statistically significant (SPSS 11.5).

### Conclusions

We discovered the prominent anti-senescence effect of ABO in cultured rat BMSCs, as evidenced by a series of senescence-associated markers. Further mechanistic investigations suggested these beneficial effects were ascribed to an improvement of cellular homeostasis primarily mediated by two novel age-associated proteins, ANXA7 and Hmbox1.

ANXA7 belongs to calcium-dependent phospholipid binding proteins, predominantly distributed in membranes in cytoplasm, and has been reported resident in endomembrane organelles, such as endoplasmic reticulum,<sup>55</sup> endosomes<sup>56</sup> and autophagosomes. However, it was the first time to observe its co-localization with lysosomes. ANXA7 could interact with other proteins and modulate phosphorylation with its GTPase activity, playing a key role in tumorigenesis, apoptosis,<sup>57</sup> autophagy<sup>29, 30</sup> and inflammation.<sup>58</sup> Based on our results, we speculated that ANXA7 probably interact with lysosomal membrane proteins, such as V-ATPase, a well-known target of Baf-A1. V-ATPase is also closely associated with aging. According to a recent study, hyperactivity of V-ATPase in yeast cells suppressed age-induced mitochondrial dysfunction, whereas V-ATPase depletion led to drastically shortened lifespan.<sup>59</sup> Therefore, lysosomal H<sup>+</sup> gradient could be considered as a key factor in cellular senescence. Whether ANXA7 participates in lysosomal H<sup>+</sup> gradient maintenance through interacting with V-ATPase needs to be further demonstrated.

Besides ANXA7, we found that ABO elevated Hmbox1 protein level which probably played a role in microfilament homeostasis. Recent studies revealed that microfilament might associate with senescence onset by modulating ROS levels<sup>60</sup> and mechanotransduction.<sup>61</sup> It was suggested that microfilaments underwent dramatical changes during aging, including assembly and organization remodeling and decreased turnover rate. We found Hmbox1 might be a novel actin-binding protein (ABP) and promote microfilament homeostasis upon ABO treatment, based on the observation of co-localization between Hmbox1 and  $\beta$ -actin. The dynamics and function of microfilament is largely dependent on its formation and assembly at cell membrane. Our result showed ABO treatment might suppress focal adhesion formation through downregulation of Caveolin-1, thus inhibiting the appearance of senescent phenotypes of microfilament and cell morphology. From this point, it would be intriguing to study the interaction between Hmbox1 and ANXA7 in microfilament homeostasis, since it was reported that annexins<sup>62</sup> were recruited to sites of actin assembly at cellular membranes and contributed to microfilament formation. Although our results indicated ANXA7 was an upstream regulator of Hmbox1 at post-transcriptional level, whether they had a direct interaction remained to be unraveled.

We were eager to know next the crosstalkings between those homeostasis maintaining effects of ABO linked by key proteins. Whether ANXA7 participated in microfilament assembly through interactions with Hmbox1, and whether Hmbox1 contributed to autophagy flux by modulating cytosolic F-actin were intriguing topics in our future study. A more thorough understanding of the molecular mechanism underlying ABO-induced anti-aging effect will provide mechanistic insight into the onset and effect of senescence in BMSCs, which will also lead to discovery of novel anti-senescence interventions with small molecules to facilitate BMSC-based therapies in regeneration medicine.

### Acknowledgements

This work was financially supported by the National Natural Science Foundation of China (No. 81321061, 91313033, J1103515, 31270877, 20972088, and 31070735) and the National 973 Research Project (No. 2011CB503906).

### Notes and references

<sup>a</sup> Institute of Developmental Biology, School of Life Science, Shandong University, Jinan 250100, P.R. China.

<sup>b</sup> The Key Laboratory of Cardiovascular Remodeling and Function Research, Chinese Ministry of Education and Chinese Ministry of Health, Shandong University Qilu Hospital, Jina, 250012, P.R. China.

<sup>c</sup> Institute of Organic Chemistry, School of Chemistry and Chemical Engineering, Shandong University, Jinan 250100, P.R. China.

\* Corresponding authors. Fax: + 86 531 88565610; Tel: + 86 531 88364929. E-mail: bxzhao@sdu.edu, miaojy@sdu.edu.cn.

† Electronic Supplementary Information (ESI) available: [details of any supplementary information available should be included here]. See DOI: 10.1039/b000000x/

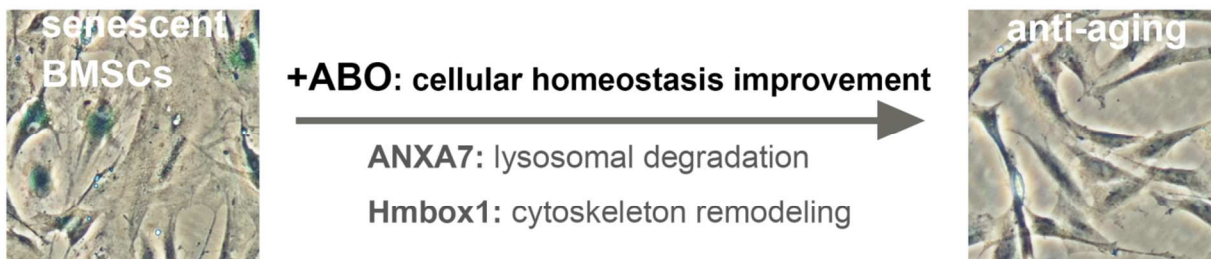
‡ Footnotes should appear here. These might include comments relevant to but not central to the matter under discussion, limited experimental and spectral data, and crystallographic data.

1. S. Forostyak, P. Jendelova and E. Sykova, *Biochimie*, 2013, **95**, 2257-2270.
2. I. K. Ko and B. S. Kim, *International journal of stem cells*, 2008, **1**, 49-54.
3. A. R. Derubeis and R. Cancedda, *Annals of biomedical engineering*, 2004, **32**, 160-165.
4. K. Stenderup, J. Justesen, C. Clausen and M. Kassem, *Bone*, 2003, **33**, 919-926.
5. M. A. Baxter, R. F. Wynn, S. N. Jowitt, J. E. Wraith, L. J. Fairbairn and I. Bellantuono, *Stem cells*, 2004, **22**, 675-682.
6. S. P. Bruder, N. Jaiswal and S. E. Haynesworth, *Journal of cellular biochemistry*, 1997, **64**, 278-294.
7. J. R. Mauney, D. L. Kaplan and V. Volloch, *Biomaterials*, 2004, **25**, 3233-3243.
8. A. Stolzing, E. Jones, D. McGonagle and A. Scutt, *Mechanisms of ageing and development*, 2008, **129**, 163-173.
9. D. Maggio, M. Barabani, M. Pierandrei, M. C. Polidori, M. Catani, P. Mecocci, U. Senin, R. Pacifici and A. Cherubini, *The Journal of clinical endocrinology and metabolism*, 2003, **88**, 1523-1527.
10. U. Galderisi, H. Helmbold, T. Squillaro, N. Alessio, N. Komm, B. Khadang, M. Cipollaro, W. Bohn and A. Giordano, *Stem cells and development*, 2009, **18**, 1033-1042.
11. D. C. Rubinsztein, G. Marino and G. Kroemer, *Cell*, 2011, **146**, 682-695.
12. A. M. Cuervo, *The journals of gerontology. Series A, Biological sciences and medical sciences*, 2008, **63**, 547-549.
13. A. M. Cuervo, E. Bergamini, U. T. Brunk, W. Droge, M. Ffrench and A. Terman, *Autophagy*, 2005, **1**, 131-140.



14. U. T. Brunk and A. Terman, *Free radical biology & medicine*, 2002, **33**, 611-619.
15. C. Song, C. Song and F. Tong, *Cytotherapy*, 2014.
16. L. Wang, X. Hu, W. Zhu, Z. Jiang, Y. Zhou, P. Chen and J. Wang, *Science China. Life sciences*, 2014, **57**, 171-180.
17. Q. Zhang, Y. J. Yang, H. Wang, Q. T. Dong, T. J. Wang, H. Y. Qian and H. Xu, *Stem cells and development*, 2012, **21**, 1321-1332.
18. Z. Chen, H. Bai, Y. Z. Pan, C. B. Wang, Q. Zhao, X. Y. Hu and X. H. Ma, *Zhonghua xue ye xue za zhi = Zhonghua xueyexue zazhi*, 2011, **32**, 602-605.
19. M. Mortensen, E. J. Soilleux, G. Djordjevic, R. Tripp, M. Lutteropp, E. Sadighi-Akha, A. J. Stranks, J. Glanville, S. Knight, S. E. Jacobsen, K. R. Kranc and A. K. Simon, *The Journal of experimental medicine*, 2011, **208**, 455-467.
20. Y. W. Eom, J. E. Oh, J. I. Lee, S. K. Baik, K. J. Rhee, H. C. Shin, Y. M. Kim, C. M. Ahn, J. H. Kong, H. S. Kim and K. Y. Shim, *Biochemical and biophysical research communications*, 2014, **445**, 16-22.
21. M. Oft, K. H. Heider and H. Beug, *Current biology : CB*, 1998, **8**, 1243-1252.
22. S. Hassane, W. N. Leonhard, A. van der Wal, L. J. Hawinkels, I. S. Lantinga-van Leeuwen, P. ten Dijke, M. H. Breuning, E. de Heer and D. J. Peters, *The Journal of pathology*, 2010, **222**, 21-31.
23. H. Tang, Y. Xiang, X. Jiang, Y. Ke, Z. Xiao, Y. Guo, Q. Wang, M. Du, L. Qin, Y. Zou, Y. Cai, Z. Chen and R. Xu, *Biochemical and biophysical research communications*, 2013, **440**, 502-508.
24. J. L. Simonsen, C. Rosada, N. Serakinci, J. Justesen, K. Stenderup, S. I. Rattan, T. G. Jensen and M. Kassem, *Nature biotechnology*, 2002, **20**, 592-596.
25. T.-J. Cho, J. Kim, S.-K. Kwon, K. Oh, J.-a. Lee, D.-S. Lee, J. Cho and S. B. Park, *Chemical science*, 2012, **3**, 3071-3075.
26. K. Johnson, S. Zhu, M. S. Tremblay, J. N. Payette, J. Wang, L. C. Bouchez, S. Meeusen, A. Althage, C. Y. Cho, X. Wu and P. G. Schultz, *Science*, 2012, **336**, 717-721.
27. L. Su, H. Zhao, C. Sun, B. Zhao, J. Zhao, S. Zhang, H. Su and J. Miao, *ACS chemical biology*, 2010, **5**, 1035-1043.
28. C. Sun, N. Wang, J. Huang, J. Xin, F. Peng, Y. Ren, S. Zhang and J. Miao, *Journal of cellular biochemistry*, 2009, **108**, 519-528.
29. L. Wang, Z. Dong, B. Huang, B. Zhao, H. Wang, J. Zhao, H. Kung, S. Zhang and J. Miao, *Autophagy*, 2010, **6**, 1115-1124.
30. H. Li, N. Liu, S. Wang, L. Wang, J. Zhao, L. Su, Y. Zhang, S. Zhang, Z. Xu, B. Zhao and J. Miao, *Biochimica et biophysica acta*, 2013, **1833**, 2092-2099.
31. P. F. Jiao, B. X. Zhao, W. W. Wang, Q. X. He, M. S. Wan, D. S. Shin and J. Y. Miao, *Bioorganic & medicinal chemistry letters*, 2006, **16**, 2862-2867.
32. Z. Dong, Y. Cheng, J. Zhao, L. Su, B. Zhao, Y. Zhang, S. Zhang and J. Miao, *Journal of cellular physiology*, 2010, **223**, 202-208.
33. L. Han, J. Shao, L. Su, J. Gao, S. Wang, Y. Zhang, S. Zhang, B. Zhao and J. Miao, *Stem cells and development*, 2012, **21**, 2762-2769.
34. A. Banfi, A. Muraglia, B. Dozin, M. Mastrogiacomo, R. Cancedda and R. Quarto, *Experimental hematology*, 2000, **28**, 707-715.
35. M. Almeida and C. A. O'Brien, *The journals of gerontology. Series A, Biological sciences and medical sciences*, 2013, **68**, 1197-1208.
36. J. Justesen, K. Stenderup, E. F. Eriksen and M. Kassem, *Calcified tissue international*, 2002, **71**, 36-44.
37. A. Muraglia, R. Cancedda and R. Quarto, *Journal of cell science*, 2000, **113 ( Pt 7)**, 1161-1166.
38. A. Bitto, C. A. Lerner, T. Nacarelli, E. Crowe, C. Torres and C. Sell, *Age*, 2014, **36**, 9626.
39. W. L. Yen and D. J. Klionsky, *Physiology*, 2008, **23**, 248-262.
40. T. Kurz, J. W. Eaton and U. T. Brunk, *Antioxidants & redox signaling*, 2010, **13**, 511-523.
41. J. Chen, S. Xavier, E. Moskowitz-Kassai, R. Chen, C. Y. Lu, K. Sanduski, A. Spes, B. Turk and M. S. Goligorsky, *The American journal of pathology*, 2012, **180**, 973-983.
42. S. Patschan, J. Chen, O. Gealekman, K. Krupincza, M. Wang, L. Shu, J. A. Shayman and M. S. Goligorsky, *American journal of physiology. Renal physiology*, 2008, **294**, F100-109.
43. S. Chen, H. Saiyin, X. Zeng, J. Xi, X. Liu, X. Li and L. Yu, *Cytogenetic and genome research*, 2006, **114**, 131-136.
44. L. Wu, C. Zhang and J. Zhang, *Cellular & molecular immunology*, 2011, **8**, 433-440.
45. L. Wu, C. Zhang, X. Zheng, Z. Tian and J. Zhang, *International immunopharmacology*, 2011, **11**, 1895-1900.
46. D. Kappei, F. Butter, C. Benda, M. Scheibe, I. Draskovic, M. Stevense, C. L. Novo, C. Basquin, M. Araki, K. Araki, D. B. Krastev, R. Kittler, R. Jessberger, J. A. Londono-Vallejo, M. Mann and F. Buchholz, *The EMBO journal*, 2013, **32**, 1681-1701.
47. X. Feng, Z. Luo, S. Jiang, F. Li, X. Han, Y. Hu, D. Wang, Y. Zhao, W. Ma, D. Liu, J. Huang and Z. Songyang, *Journal of cell science*, 2013, **126**, 3982-3989.
48. M. N. Starodubtseva, *Ageing research reviews*, 2011, **10**, 16-25.
49. I. Sokolov, S. Iyer and C. D. Woodworth, *Nanomedicine : nanotechnology, biology, and medicine*, 2006, **2**, 31-36.
50. G. Kasper, L. Mao, S. Geissler, A. Draycheva, J. Trippens, J. Kuhnisch, M. Tschirschmann, K. Kaspar, C. Perka, G. N. Duda and J. Klose, *Stem cells*, 2009, **27**, 1288-1297.
51. S. Tojkander, G. Gateva and P. Lappalainen, *Journal of cell science*, 2012, **125**, 1855-1864.
52. K. A. Cho, S. J. Ryu, Y. S. Oh, J. H. Park, J. W. Lee, H. P. Kim, K. T. Kim, I. S. Jang and S. C. Park, *The Journal of biological chemistry*, 2004, **279**, 42270-42278.
53. M. F. Pittenger, A. M. Mackay, S. C. Beck, R. K. Jaiswal, R. Douglas, J. D. Mosca, M. A. Moorman, D. W. Simonetti, S. Craig and D. R. Marshak, *Science (New York, N.Y.)*, 1999, **284**, 143-147.
54. F. W. Wang, S. Q. Wang, B. X. Zhao and J. Y. Miao, *Organic & biomolecular chemistry*, 2014, **12**, 3062-3070.
55. C. S. Clemen, A. Hofmann, C. Zamparelli and A. A. Noegel, *Journal of muscle research and cell motility*, 1999, **20**, 669-679.
56. M. Marko, Y. Prabhu, R. Muller, R. Blau-Wasser, M. Schleicher and A. A. Noegel, *European journal of cell biology*, 2006, **85**, 1011-1022.
57. C. Guo, S. Liu, F. Greenaway and M. Z. Sun, *Clinica chimica acta; international journal of clinical chemistry*, 2013, **423**, 83-89.
58. G. Badalian, B. K. Kurbanmuradov, V. G. Poliakov and Z. S. Ordukhaniyan, *Pediatrics*, 1990, 100-102.
59. A. L. Hughes and D. E. Gottschling, *Nature*, 2012, **492**, 261-265.
60. M. E. Farah, V. Sirotkin, B. Haarer, D. Kakhniashvili and D. C. Amberg, *Cytoskeleton*, 2011, **68**, 340-354.
61. M. Wu, J. Fannin, K. M. Rice, B. Wang and E. R. Blough, *Ageing research reviews*, 2011, **10**, 1-15.
62. U. Rescher and V. Gerke, *Journal of cell science*, 2004, **117**, 2631-2639.

## Table of Content



ABO was discovered as a novel anti-aging chemical in cultured BMSCs by improving intracellular homeostasis.